


## Article

# The Influence of Integral Water Tank on the Seismic Performance of Slender Structure: An Experimental Study

Bing Xu <sup>1,\*</sup> , Zhenyu Han <sup>1,2</sup>, Lang Wang <sup>1,3</sup>, Qin Liu <sup>1,3</sup>, Xueyuan Xu <sup>1,4</sup> and Huihui Chen <sup>5</sup><sup>1</sup> College of Civil Engineering, Yancheng Institute of Technology, Yancheng 224051, China<sup>2</sup> School of Electricity Power Engineering, Kunming University of Science and Technology, Kunming 430074, China<sup>3</sup> School of Civil Engineering & Architecture, Anhui University of Science & Technology, Huainan 232001, China<sup>4</sup> Key Laboratory of Navigation Structures Technology, Ministry of Transport, Nanjing Hydraulic Research Institute, Nanjing 210029, China<sup>5</sup> Department of Civil Engineering, Yancheng Polytechnic College, Yancheng 224001, China; chh1990803@163.com

\* Correspondence: bateren@126.com

**Abstract:** The slender structure is prone to be affected by horizontal force; therefore, the seismic performance needs to be considered carefully. Meanwhile, due to the low cost and good performance on the seismic resistance of the Tuned liquid dampers (TLDs) system, it has been widely used for vibration control. Regarding the abovementioned background, in this study, we conduct the experiment to investigate the seismic performance of the slender structure with the integral water tank, and two designed parameters (the placement location and the water level of the water tank) are studied. The experimental phenomenon and the structural accelerations are recorded to be analyzed further and discussed, then a useful design guide for an integral water tank is summarized. Finally, some practical and helpful advice and conclusions are put forward for the design of the water tank that is used for the purpose of seismic resistance in the slender structure. Our research can fill the blank in the research on the integral water tank of TLDs system, which also has good potential to achieve the enhancement of slender structure seismic performance.



**Citation:** Xu, B.; Han, Z.; Wang, L.; Liu, Q.; Xu, X.; Chen, H. The Influence of Integral Water Tank on the Seismic Performance of Slender Structure: An Experimental Study. *Buildings* **2023**, *13*, 736. <https://doi.org/10.3390/buildings13030736>

Academic Editor: Hongfei Chang

Received: 26 January 2023

Revised: 3 March 2023

Accepted: 8 March 2023

Published: 10 March 2023



**Copyright:** © 2023 by the authors. Licensee MDPI, Basel, Switzerland. This article is an open access article distributed under the terms and conditions of the Creative Commons Attribution (CC BY) license (<https://creativecommons.org/licenses/by/4.0/>).

**Keywords:** integral water tank; slender structure; seismic performance; seismic design; Tuned liquid dampers (TLDs) system

## 1. Introduction

Tuned liquid dampers (TLDs), as a widely used sloshing tank damper, achieve a successful application in the energy dissipation and vibration control of the building [1–5]. The main component of TLD is a fixed integral water tank that placed on the structure; when the horizontal external force is applied to the structure, the horizontal displacement emerges and then causes the sloshing of the water in the tank, further leading to the wave with phase difference of around 90° comparing to the structure vibration [6–8], so that the impact of wave on the structure is used to resist the external excitation to achieve the purpose of seismic resistance [9,10]. The widely used water tanks are of circular, rectangular or ringlike shapes [11–14], placed on the top floor to control the wind load and earthquake that applies to the structure [15], because the device of TLD only relies on the internal liquid rather than additional external energy, which is regarded as an economical and effective vibration reduction measures [16].

The basic vibration reduction principle of the TLD can be explained in the following way. When the structural vibration occurs to cause the displacement of the device of TLD, further to make the internal liquid slosh [17], the vibration energy is dissipated through the friction and wave motion between the liquid and the structure [18]. Such dynamic

process includes the accumulation between structural restoring force and liquid sloshing load [19,20]. Following the principle, Vandiver and Mitome [21] first adopted the oil storage tank on an offshore platform as the device of TLD to analyze the dynamical responses of the platform under the condition of wave loading, which primarily validates the performance of seismic resistance of TLD. Due to the results of the abovementioned work, such device is gradually adopted by some researchers to achieve the seismic resistance of ground structures [22–26]. In the study by Kareem and Sun [26], the random seismic response analysis of the TLD-structure system was conducted based on the simulation of the ground motion of a stationary and non-stationary stochastic process. Then, the researchers in Refs. [27,28] aimed at the investigation of effects of vibration reduction in TLD device. First, the responses of TLD-structure system under wind and harmonic loads were calculated, while the experiment on the water tank was also conducted. Roy et al. [29] adopted the way of laboratory experiment, and reported the TLD device with shallow liquid illustrated better performance of seismic resistance in the situation of structural vibration with a small amplitude. After that, the energy dissipation of elevated water tanks and similar structures was also achieved based on TLD passive damping technology [30]. Furthermore, Ocak et al. [31] exploited the optimization algorithm to determine the liquid of the TLDs system to make the liquid able to absorb the energy, leading to better damping performance. In the study of Zhang [32], the nonlinear reduced-order model was proposed to explain the nonlinear behavior of the TLDs, the research also considered the shallow and deep water levels. Moreover, Kamgar et al. [33] aimed at the single-degree-of-freedom system with a modified TLD. The interaction between the soil and structure was investigated, and the results illustrate that the modified TLD can reduce the reaction well. Ref. [34] developed a friction pendulum-strengthened TLD and deduced the corresponding analytical model. The finite element method was used to validate the proposed model, and the outcomes can provide good guidance for the multiple seismic performances of a base-isolated structure. In addition, Hsieh et al. [35] conducted a numerical study on the Tuned mass damper (TMD) and TLD to determine the hybrid performance on the vibration control. The results prove the hybrid TMD and TLD system is of great potential for the application of floating offshore structures. The abovementioned studies pointed out the superiority and the potential of the TLD-structure system for the seismic resistance, but several key issues still need to be solved, such as the fact that (1) the adopted water volume in the TLD has been not investigated well; (2) the optimal placement of the TLDs system needs to be evaluated for the better seismic performance; (3) instead of the qualitative work, more quantitative study is needed. These problems have set some barriers to the development and application of TLDs in the practical engineering structure, therefore, more attention should be paid to this field.

Due to the low cost and good performance on the seismic resistance of the TLD system, in this study, we adopt the placement location and the water level of the tank as the variables, the structural dynamic features (including accelerations of the structure and water sloshing characteristics); the observed phenomena are monitored in the experiment, then the variable analysis is conducted to investigate the influence of the integral water tank on the seismic performance of the slender structure.

The remaining sections are organized as follows: Section 2 describes the basic damping theory of integral water tank and the experimental design; Section 3 summarizes the observed experimental phenomenon. Then, we analyze the obtained experimental phenomenon and results in detail; after that, the useful design guide for the integral water tank is proposed in Section 5. Finally, based on the aforementioned contents, we draw several conclusions and outlooks in Section 6.

## 2. Theoretical Background and Experiment Setup

The slender structure has been widely used in practical engineering. However, environmental conditions, such as wind and earthquake, cause the vibration of the engineering structure. In this section, first, the damping theory of the water tank is introduced based on

the structural dynamics and fluid dynamics. Then, we design an experimental model of a slender structure with an integral water tank for the subsequent research. The details are described in the following sections.

### 2.1. Damping Theory of Integral Water Tank

When the external excitation is applied to the tank that is filled with water, the vibration of the tank causes a sloshing in the water. Then, due to the inertia force, a phase difference occurs between the movements of the water body and the structure. As shown in Figure 1, the emerged inertia force in the water is determined by the mass of the water and the acceleration of the tank. According to structural dynamics, the motion equation of the structure can be written as follows:

$$Kx(t) + C\dot{x}(t) + M\ddot{x}(t) = P(t), \quad (1)$$

where  $K$ ,  $C$  and  $M$  stand for the stiffness, damping and mass matrix of the structure, respectively;  $x$ ,  $\dot{x}$  and  $\ddot{x}$  represent the displacement, velocity and acceleration of the structure; and  $P$  can be explained as the external excitation.

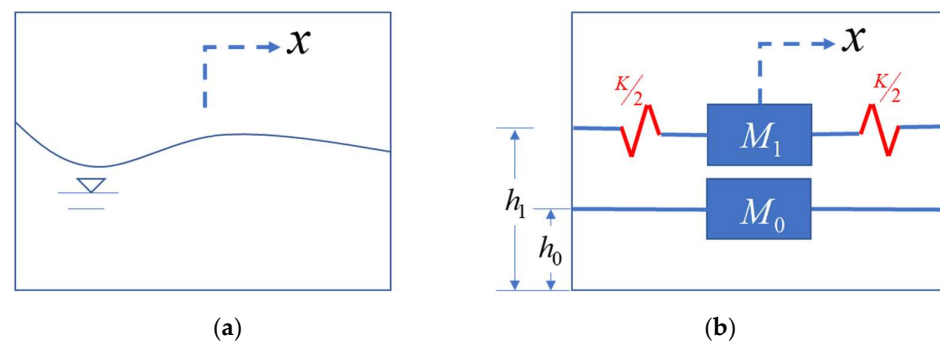


**Figure 1.** The simplified model of damping theory under the variation on water level. (a) The change characteristics of water level motion. (b) The simplified mechanical model of water sloshing.

When the integral water tank is placed in the structure, the existence of the tank changes the damping of the original structure, further to alter the motion status. Regarding this situation, the abovementioned motion equation can be written as follows:

$$\omega_n^2 x(t) + 2\zeta_n \omega_n \dot{x}(t) + \ddot{x}(t) = P'(t), \quad (2)$$

where  $\omega_n$  is the  $n$ -th circular frequency;  $\zeta_n$  stands for  $n$ -th damping ratio, which can be defined as 0.05 according to Ref. [25]; and  $P'(t) = P(t) - F_w$  can be expressed as the external excitation that is influenced by the inertia force in the water. Then, referring to the fluid dynamics, the dynamic coefficient of the sloshing water body caused by the structural vibration can be expressed as follows:

$$\begin{aligned} F_w &= m_w \sum_{n=1}^{\infty} \alpha_n \omega_n^2 + \beta_n m_w \ddot{x}_g \\ \omega_n^2 &= \frac{(2n-1)g\pi}{L} \tanh \frac{(2n-1)h\pi}{L} \\ \alpha_n &= \frac{8L}{(2n-1)^3 \pi^3 h} \tanh \frac{(2n-1)h\pi}{L} \\ \beta_n &= 1 - \sum_{n=1}^{\infty} \alpha_n \end{aligned} \quad (3)$$

where  $m_w$  represents the mass of the water;  $\omega_n$  means the  $n$ -th circular frequency of the structure influenced by the sloshing water, which can be obtained based on Housner theory;  $g = 9.8 \text{ m/s}^2$ , is the gravitational acceleration;  $h$  is the water level in the tank;  $L$  and  $\ddot{x}_g$

indicate the length of the tank and the acceleration of the water tank placement floor along the vibration direction, respectively.

## 2.2. The Design of Experimental Model

For the purpose of investigating the influence of integral water tanks on the seismic performance of the slender structure, in this section, we adopt a 5-storey experimental structure with a width–height ratio of 10:1; the design drawing of the model is illustrated in Figure 2a. The experimental structure is constructed on the steel frame, each floor slab is fixed with the column by bolt riveting. The integral water tank is an acrylic rectangle tank of 22 cm × 22 cm × 25 cm, and the thickness of acrylic plate used for water tank fabrication is 1 cm; for convenient observation, we draw a grid with an interval of 2 cm on the side of the tank (Figure 2c). Then, we consider the different tank placements and the variable water levels to determine diverse experimental cases. The site of the tank is changed from the second to the top floor, and the water level can be selected from 0 cm to 8 cm with an interval of 2 cm. After that, the external excitation is first applied to the structure to generate initial vibration, meanwhile accelerations on the top floor and in the floor with the tank are collected by the sensors at a sampling rate of 1000 Hz (Figure 2b). Moreover, the sloshing form of the water during the structural vibration is recorded using the video camera. It should be noted that for better observation and collection of the sloshing characteristics, the filmed photos are gathered based on repeatable experiments.

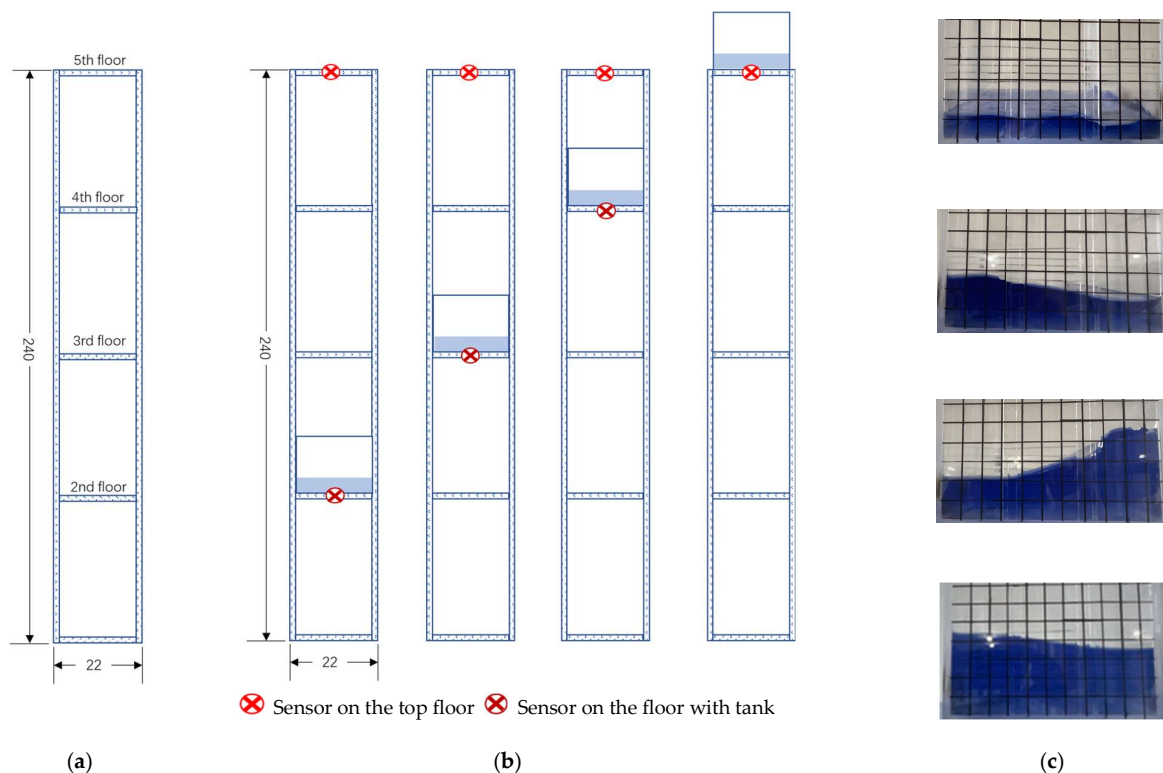


**Figure 2.** The overall drawing of the experimental model. (a) The overall. (b) Placement scheme of integral water tank. (c) The integral water tank with different water levels when water sloshes on the top floor.

## 3. The Description of Experimental Phenomenon

In this section, the sloshing process of the water in the tank is described in detail. At first, the free vibration emerges in the structure due to the external excitation; then, the free vibration causes the water to slosh simultaneously, and the repeated sloshing of the water functions in the structure like a damping system to dissipate energy; finally, the vibration

and sloshing achieve a resonance situation and keep a synergetic shaking until the energy dissipates totally.

Aiming at the different water levels, Figures 3 and 4 illustrate the water oscillation forms in the sloshing process and in resonance status, respectively. It should be pointed out that all photos were captured when the tank was placed on the top floor due to the limited intensity of external excitation. Meanwhile, during the sloshing process, it can be seen that the placement has a poor influence on the water oscillation forms under the same water level; namely we can observe similar water oscillation forms in the same water level, regardless of the placement. However, the unequal energy of different floors causes a difference in the sloshing amplitude of the water.

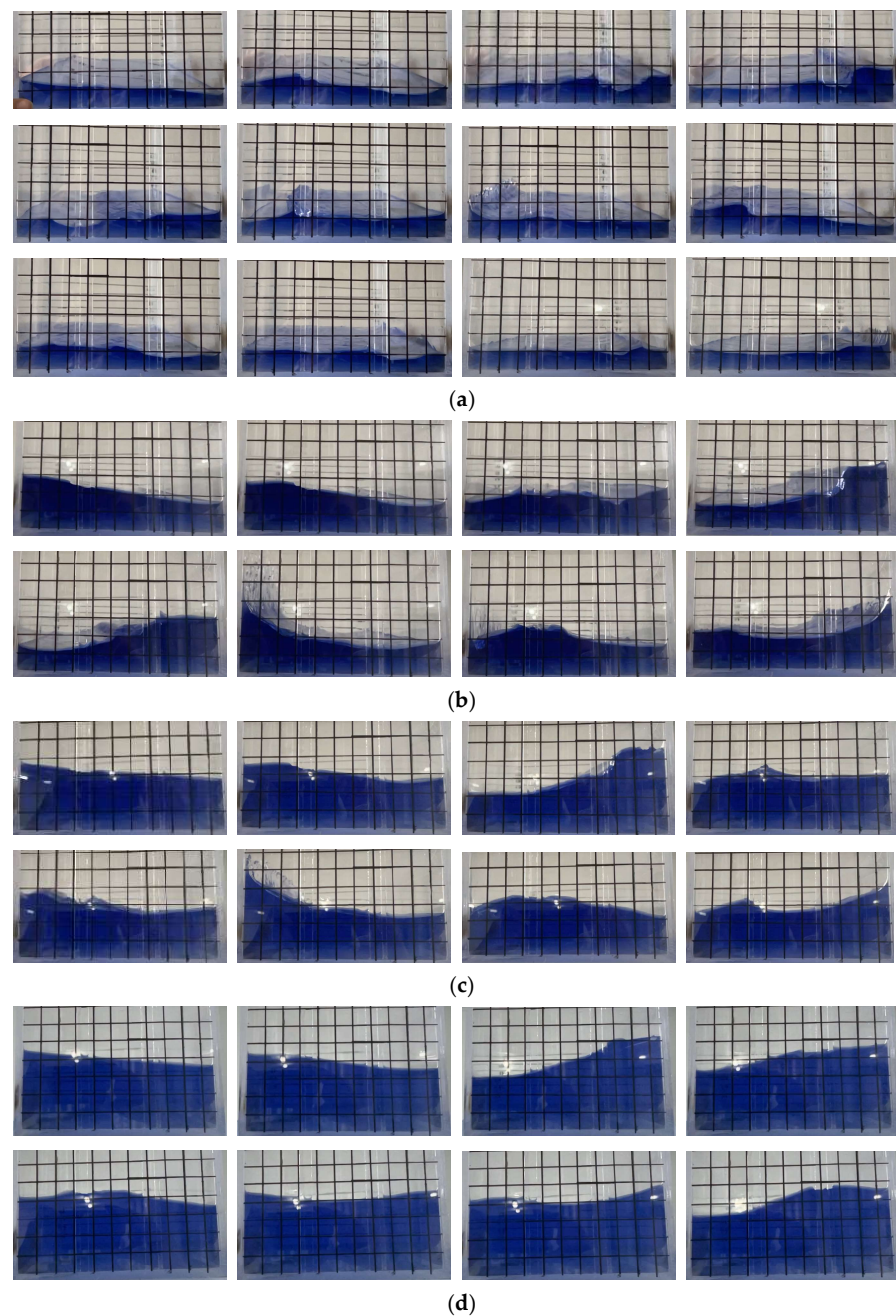


**Figure 3.** Water oscillation forms in sloshing process of different water levels. (a) Water level of 2 cm. (b) Water level of 4 cm. (c) Water level of 6 cm. (d) Water level of 8 cm.

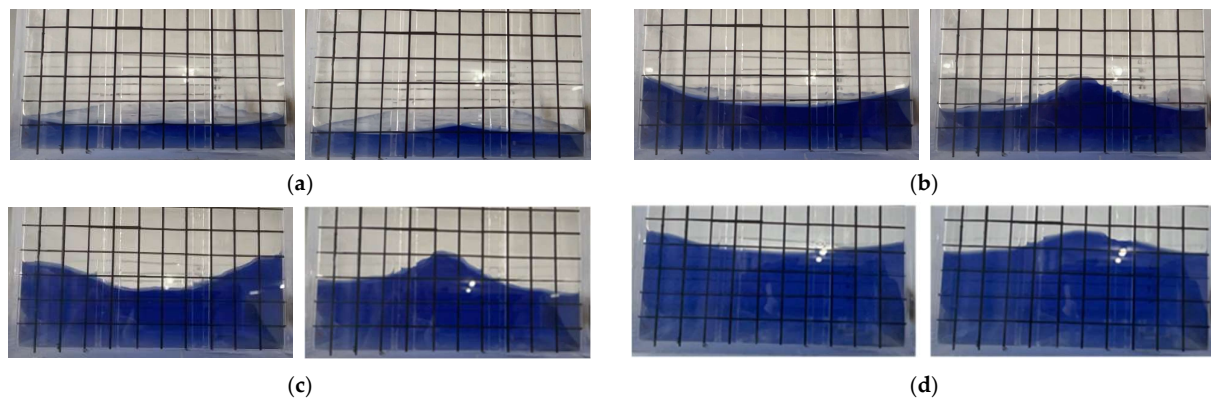


**Figure 4.** Water oscillation forms in resonance status of different water levels. (a) Water level of 2 cm. (b) Water level of 4 cm. (c) Water level of 6 cm. (d) Water level of 8 cm.

Meanwhile, from the video recording, it can be seen that after the emergence of the first sloshing in the water tank with a water level of 2 cm, the tank starts to show the same motion direction as the structure; therefore, due to the existence of inertia, we can observe a sloping water surface in the tank, and the surface in the ahead-of-motion direction is slightly lower than the back one; the discrepancy is approximately half a grid. Then, when the structure achieves the max vibration amplitude, the phase difference caused by the inertia makes the straight line of the water level become a curve, as well as causes the swell in the back. After that, the swell moves along the motion direction of the structure to form two crests in the tank, and the swell occurs again when the first of the two crests arrive at the front plate, but the swell height rises to the height of approximately one grid. Furthermore, accompanying the process of the swell in the front beginning to move to the back plate, there are a total of three crests in the tank; at the same time, the swell in the back plate is moving to the middle. Then, the swells in the front and the back meet in the 1/3 of the tank first to form an impact wave with a height of 2 cm, and then the impact wave hits the back plate to cause a swell with a height of 3 cm. Next, with the change in structure movement direction, the swell with a height of 3 cm transfers to the front plate. In addition, due to the reaction between the reflecting wave and the swell in the back as well as the generated new swell, the height of the subsequent swell is lower than that of the first one. Finally, the energy dissipation makes the water surface keep shaking up and down steadily.

In the case of the water tank with a water level of 4 cm, after the first sloshing emerges on the water, the water surface illustrates a steady variation, namely the surface that is close to the motion direction is slightly higher than the surface in the back; when the structure achieves the max vibration amplitude, the swell with a height of around half grid has occurred in the back plate. Then, the motion direction of the structure is changed, so that the swell starts to move to the front plate. Two crests can be observed in the tank; when two crests hit the front plate, the swell with a height of approximately two grids occurs and then moves to the back accompanying the motion direction of the structure, which alters simultaneously. After that, the swell arriving at the back plate results in the impact wave with a height of approximately five grids, and the impact wave returns to the front plate with the motion direction change in the structure again. However, when the swell returns to the back plate for the second time, the height of the impact wave is reduced to the two-and-a-half-grid size and produces no splash.

Regarding the water tank with a water level of 6 cm, it illustrates a similar sloshing situation to the one with a water level of 4 cm. The swell and impact wave in the back and front plates both show good consistency to the water tank with a water level of 6 cm. However, for the water tank with a water level of 8 cm, the sloshing process only shows the swell in the front and back plates; then, the water achieves the resonance status, and there is no obvious wave impact and splash occurring in the water surface.

Figures 5–8 depict the measured acceleration responses of top floor and tank floor when the water tank with different water levels is placed on different floor of the structure, and Table 1 lists the max acceleration amplitude corresponding to every acceleration response. From the figures, it can be seen that (1) the vibration of each floor is reduced due to the placement of the water tank, and the max amplitude of acceleration shows a declining trend over time, which means the damping that formed by the water exerts a negative effect on the structural vibration; (2) after the external excitation is applied to the structure, the peak points of acceleration responses emerge in the first wave crest or trough as well as the swell phenomenon in the back plate. After that, when the accelerations show another wave trough or crest, the swell occurs in the front plate. The height of such swell is higher than that of the first one in the back plate, and the peak of acceleration response is also smaller than that of the first response; (3) Table 1 demonstrates that the increased placement height of the water tank reduces the gap between the acceleration peak points in two measurement points; in addition, the alpha, namely the ratio between the measured max acceleration amplitudes of top floor and tank floor, shows a correlation with the tank placement floor (Figure 9), which means the structural dynamical responses are related to the location of tank placement. Furthermore, regarding each condition of tank placement floor, the mathematical relationship between the alpha and the water level can be obtained by the linear fitting.

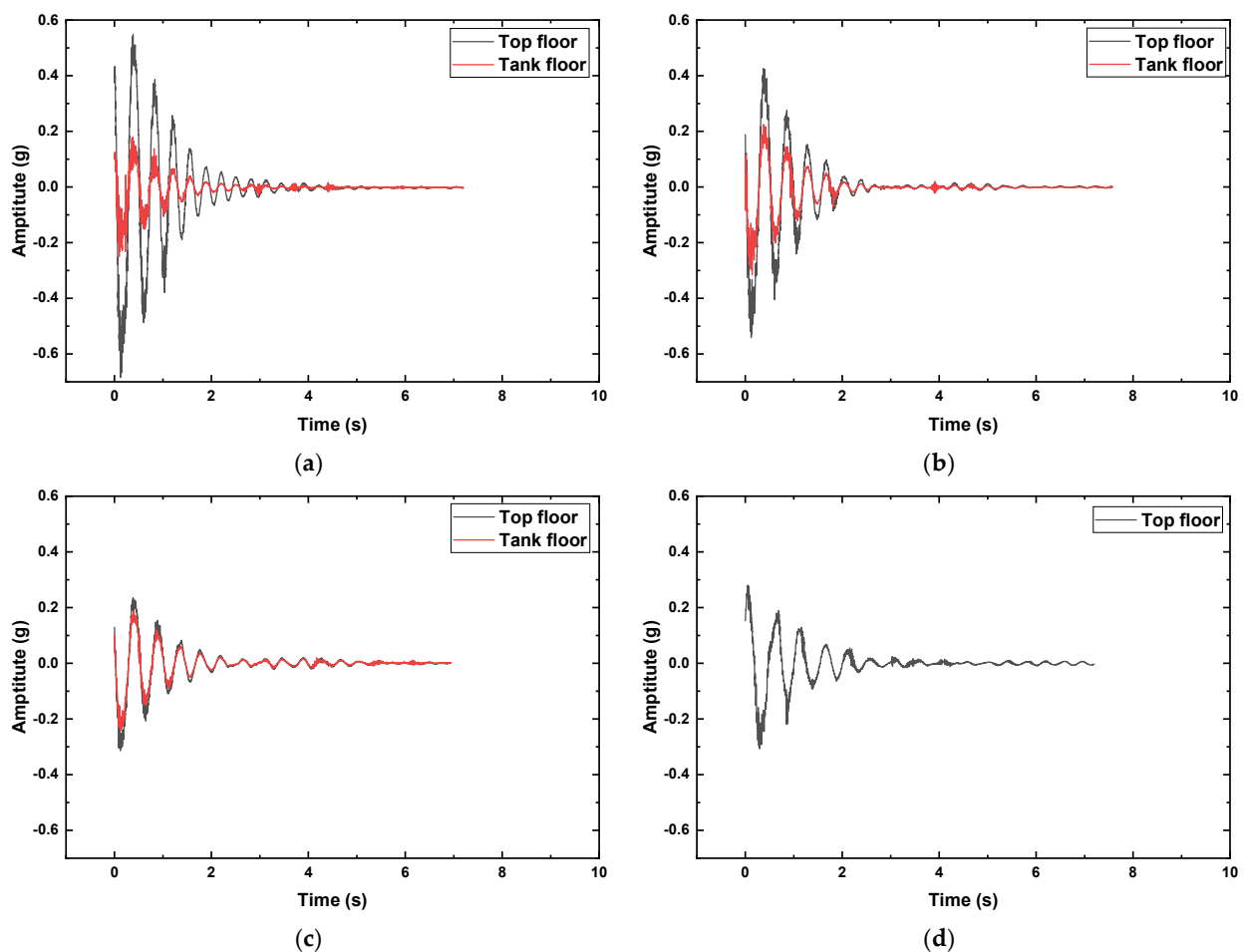


**Figure 5.** The accelerations when the water tank with a water level of 2 cm is placed on each floor of the structure. (a) 2nd floor; (b) 3rd floor; (c) 4th floor; (d) 5th floor.

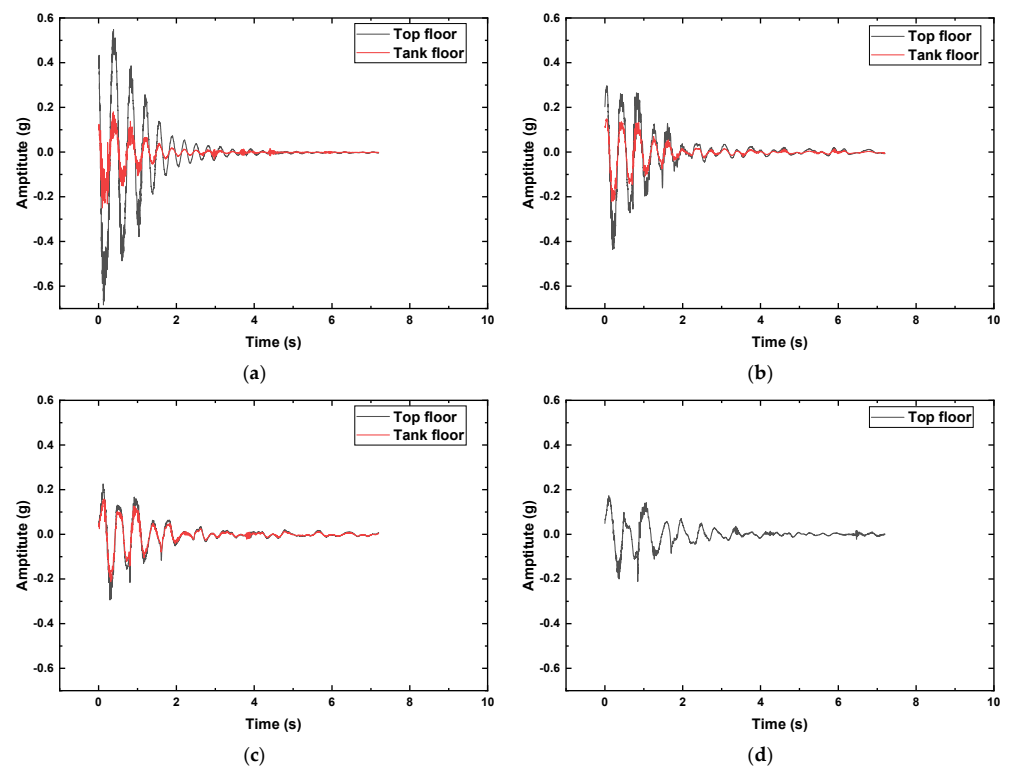


**Figure 6.** The accelerations when the water tank with a water level of 4 cm is placed on each floor of the structure. (a) 2nd floor; (b) 3rd floor; (c) 4th floor; (d) 5th floor.

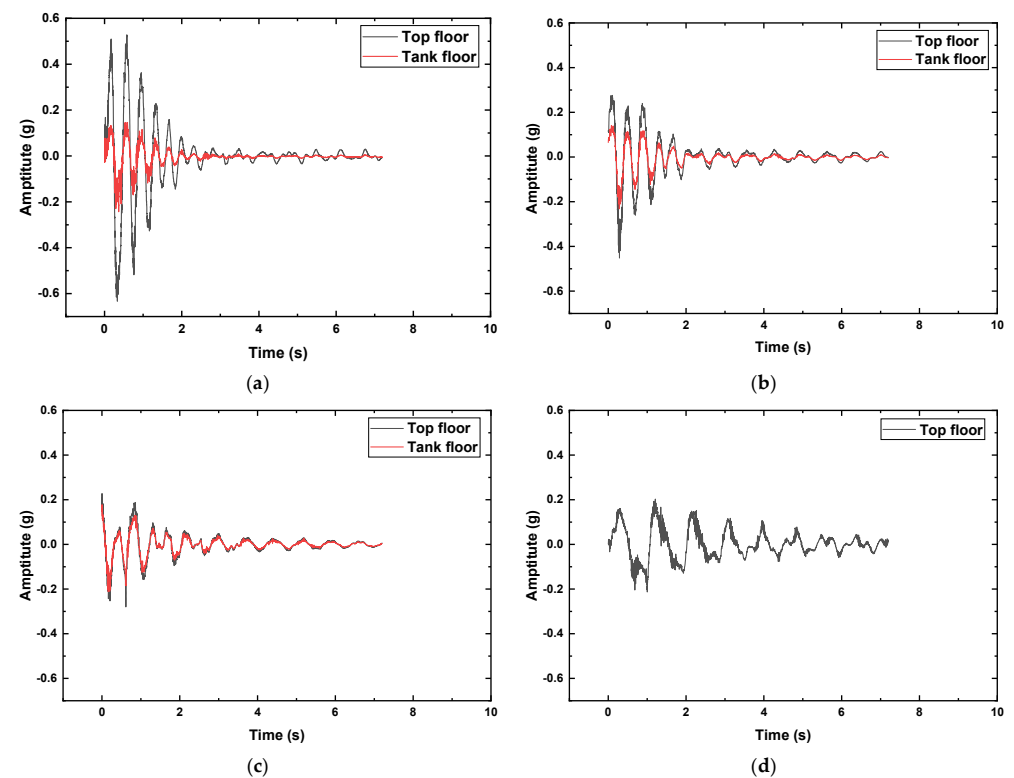


**Figure 7.** The accelerations when the water tank with a water level of 6 cm is placed on each floor of the structure. (a) 2nd floor; (b) 3rd floor; (c) 4th floor; (d) 5th floor.



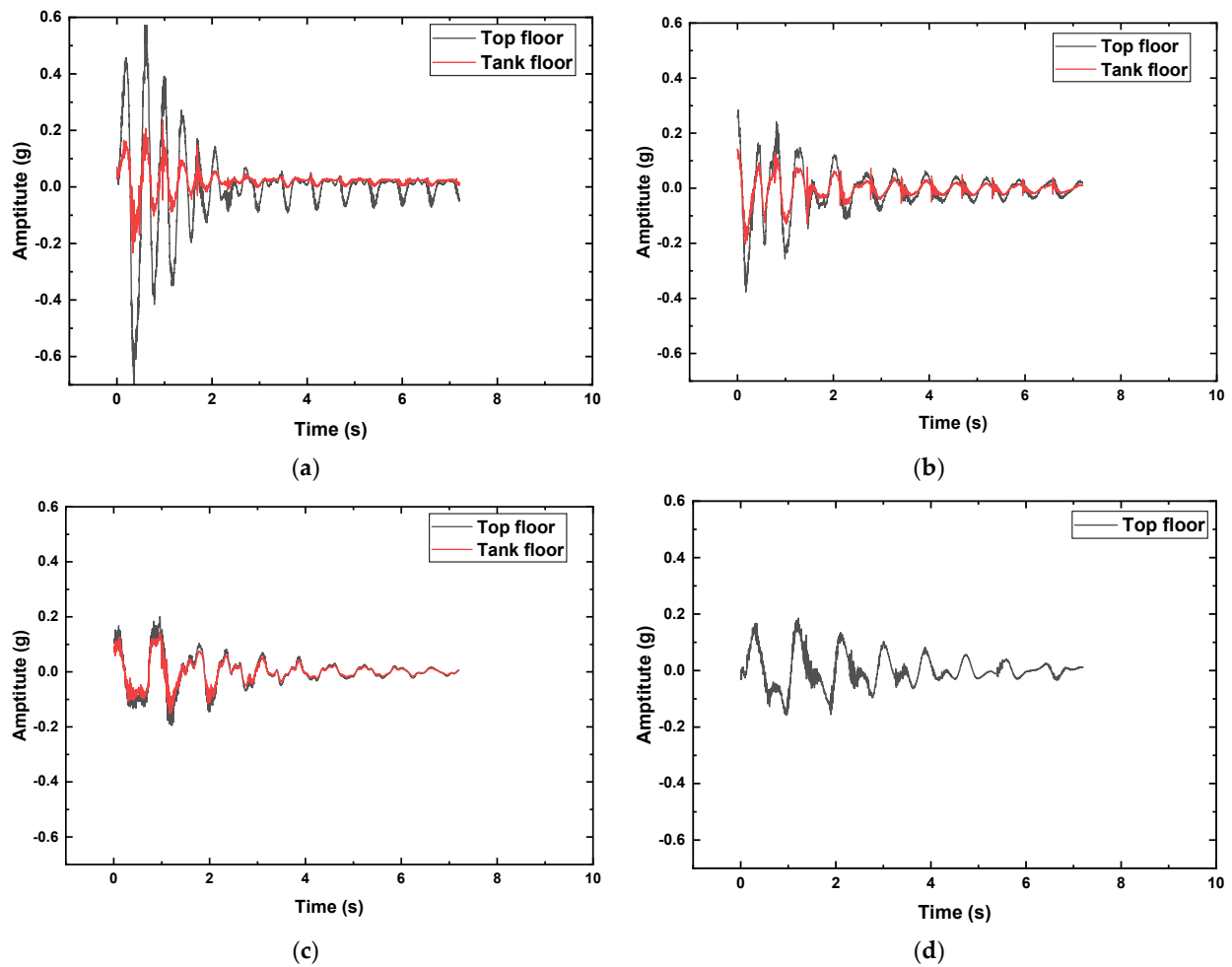


**Figure 8.** The accelerations when the water tank with a water level of 8 cm is placed on each floor of the structure. (a) 2nd floor; (b) 3rd floor; (c) 4th floor; (d) 5th floor.

**Table 1.** The max acceleration amplitude considering the water tank with different water level placed on the different floor.

Sensors Location	Water Level/cm	Location of Water Tank Placement		
		2nd Floor	3rd Floor	4th Floor
Top floor	2	0.51	0.358	0.224
Tank floor		0.157	0.188	0.17
Alpha		0.307843	0.52514	0.758929
Top floor	4	0.54	0.256	0.129
Tank floor		0.11	0.106	0.101
Ratio		0.203704	0.414063	0.782946
Top floor	6	0.421	0.205	0.141
Tank floor		0.116	0.109	0.099
Alpha		0.275534	0.531707	0.702128
Top floor	8	0.411	0.165	0.198
Tank floor		0.135	0.086	0.133
Alpha		0.328467	0.521212	0.671717
Top floor	0	0.379	0.424	0.401
Tank floor		0.102	0.224	0.334
Alpha		0.269129	0.528302	0.832918

Note: Alpha = top floor/tank floor.

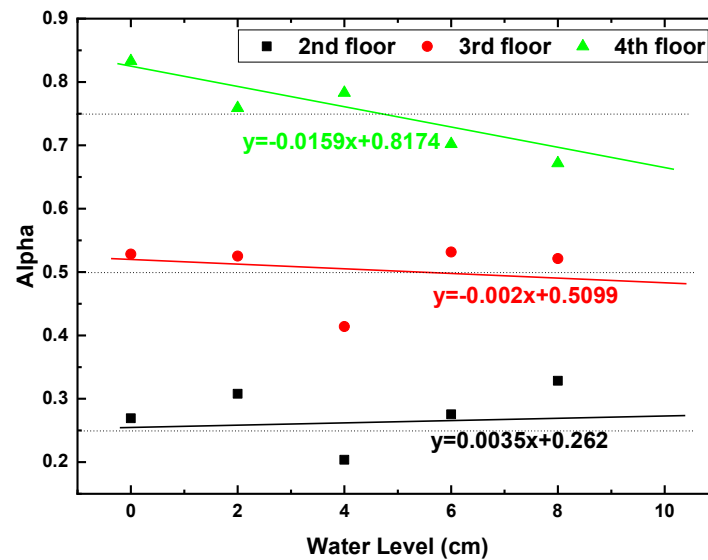


Figure 9. The ratio between the measured max acceleration amplitudes of top floor and tank floor.

#### 4. The Analysis and Discussion on the Results

##### 4.1. The Placement Location

As shown in Figures 5–8, it can be seen that the different placement of the water tank can cause a serious influence on the measured accelerations; the higher placement of the water tank, the more unstable the peak of the acceleration curve, especially for when the tank is placed on the top floor, except the situation of the tank with a water level of 2 cm. The acceleration curves of other tanks all illustrate periodic wave with multiple peaks instead of harmonic wave (Figure 10); for the occurrence of periodic wave with multiple peaks, such phenomenon can be owed to the impact caused by the swell hitting the plate of the tank, applying some effects on the peaks of the original wave.

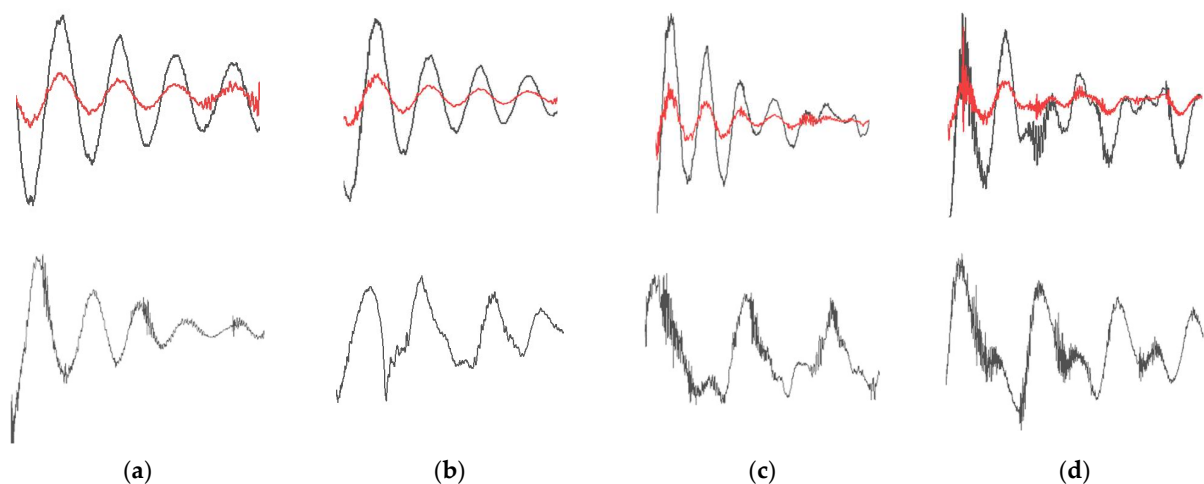
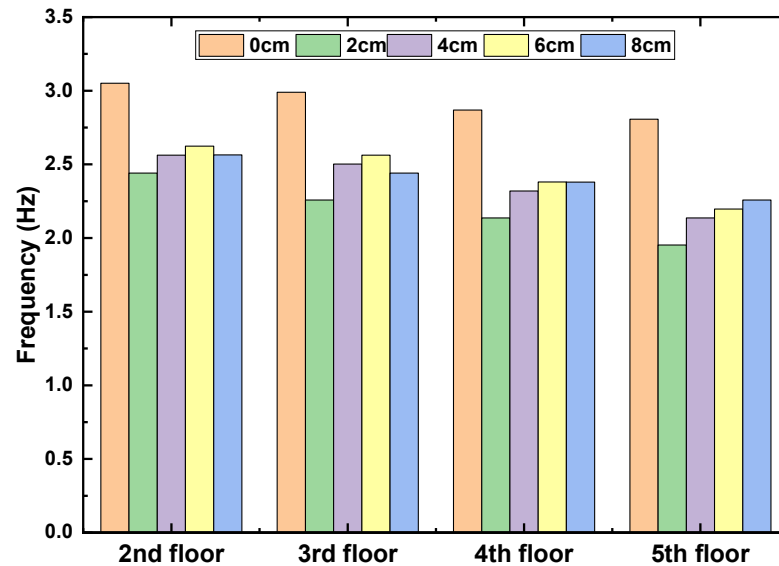


Figure 10. The changes in the forms of acceleration curves when the tank is placed on the top floor. (a) 2 cm; (b) 4 cm; (c) 6 cm; (d) 8 cm.

Then, we extract the corresponding natural frequencies of each acceleration response and plot them in Figure 11. From the obtained results, it can be seen that regardless of the placement location, the first natural frequencies of the structure without the water tank are all higher than the structures with the water tank, which means the existence of the water can change the total mass of the original, leading to variations in the frequencies. Meanwhile, with the alternation in the placement, the corresponding frequencies also

have been reduced, which means the diverse placement of water tank will affect the distribution of the structural stiffness. The change relation can be summarized as the ascendant placement height of the tank can reduce the stiffness further to lead to the decrease in the frequencies.



**Figure 11.** The first natural frequency of the structure when the water tank with a different water level placed on the different floor.

The results of Figures 5–8 demonstrate that the damping formed by the water affects the forms of structural acceleration curves. When the water tank is installed on the middle floor of the structure, the measured acceleration curve on the tank floor shows a violent shake in the corresponding peak location, but the curve on the top floor is stable. After several seconds, the discrepancy of the two curves is gradually reduced, which indicates the water tank functions as a damping system to cause the change in the structural vibration form and dissipation in the energy, finally resulting in the stable resonance status of Figure 4.

For the purpose of study on the damping ratio quantitatively, we adopt the damping ratio calculated equation, which can be written as follows:

$$\zeta = \frac{1}{j2\pi} \ln \frac{A_{i+j}}{A_i}, \quad (4)$$

where  $A_i$  means the acceleration amplitude corresponding to the  $i$ -th peak of the acceleration and  $A_{i+j}$  stands for the acceleration amplitudes corresponding to the  $i$ -th to  $j$ -th peaks of the acceleration. Then, the obtained results are plotted in Figure 12. From the figure, we can observe that the existence of the water tank can enhance the calculated damping ratio regardless of the measurement point [30]; at the same time, with the increased height of the tank placement, the calculated damping ratio based on the acceleration that is collected from the tank floor is also raised. However, for the obtained damping ratio based on the acceleration that is collected from the top floor, the curves of the calculated damping ratio first go up, and then decline for the water tank with water levels of 0 cm, 6 cm and 8 cm. Regarding the water level of 2 cm, it proceeds in an ascending trend. The curve of the water level of 4 cm first illustrates a decrease, then a rise. In addition, it should be noted that the average damping ratio of top floor is max one.

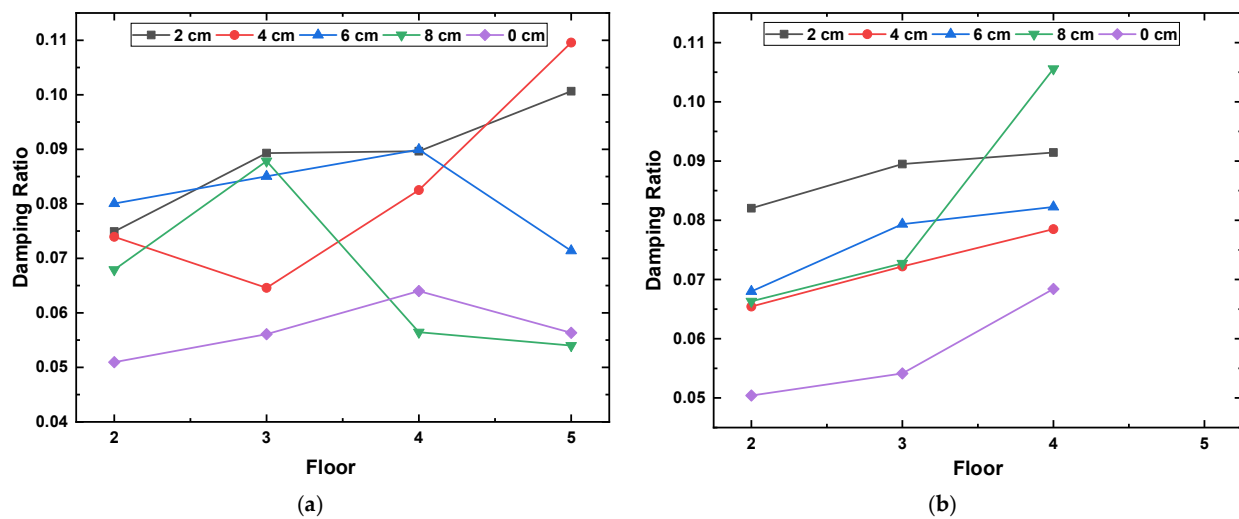


**Figure 12.** The calculated damping ratio based on the measured accelerations. (a) Top floor measurement; (b) Tank floor measurement.

#### 4.2. Height of the Water Level

From the obtained accelerations, we can also see that the increased water level transforms the stable harmonic wave form of the original signal to the periodic wave. This situation can be investigated by the video record playback. It is determined that when the wave form of the measured acceleration is changed, the reaction between the swell and plate in the tank emerges. Such process dissipates the energy to cause the occurrence of the change.

Meanwhile, from Table 1 and Figures 5–8, it can be determined that when the tank is located in the bottom of the structure, there is an obvious difference in amplitude between the top floor and tank floor. Such discrepancy accounts for the 1/4 of amplitude on the top floor, while with the increase in the water level, the gap narrows slightly. The change relationship is depicted in Figure 9. For the tank that is installed on the high top, the alpha value declines with the increase in the water level.

Regarding the damping ratio curve, it can be seen that when the tank is located in the 2–4th floors, the shallow water level ( $h = 2$  cm) can achieve a higher damping than the other levels, but the tank with a water level of 4 cm can lead to the maximum, followed by the 2 cm, and 8 cm, and 0 cm, the latter two presenting with approximately the same ratios when the tank is placed on the top floor. In conclusion, the abovementioned findings also show good consistency with the existing conclusions of other similar studies, demonstrating namely that the shallow water tank in the structure shows better seismic performance than the deep one.

#### 4.3. The Sloshing Characteristics of the Water Surface

From Figure 3, it can be observed that in the tank with a shallow water level ( $h = 2$  cm), the multiple swells can be excited during the sloshing process, and the height of the back swell is higher than that of the front one, both of which move along the vibration direction. Then, regarding the first stage, the spray is mainly the form of swell accompanied by the energy accumulation. After a period of the structural vibration, the front reflected crest hits the back one and then breaks, and the back crest impacts the front plate with high energy. Such splash emerged in this process, far higher than the water level. Furthermore, for the water tank with a water level of 4 and 6 cm, the situations of swell and impact also occurred, as well as the higher splash, but the emerged crest was always single. Moreover, the swell accounts for the water tank with a water level of 8 cm, and the height of swell is weaker than that of the others. We can observe the final water oscillation forms of the water

tank with diverse water levels in Figure 4, which indicates the water tank with different water levels demonstrates the approximately consistent stable water oscillation status.

### 5. The Design Guide for Integral Water Tank Damping System

Based on the experimental phenomenon and the investigation of the designed parameters, the water level in the water tank does not display a positive correlation with the effects of vibration energy dissipation. For the slender structure, the excess of water in the tank is likely to cause the burden of excessive weight on the top floor. Meanwhile, it can be observed that the vibration energy is dissipated by the water swell, wave impact and plate impact, and with higher placement of the water tank, more damping is applied to the structure, as well as effects on the vibration amplitude. It is advised to install the tank in the middle and upper part of the structure, namely  $3/4$  to  $1$  of the overall height is optimal.

However, for the study on the damping, the generated damping effect does not always benefit from the increased water level. The obtained experimental data and the theory of shallow water sloshing energy absorption can be utilized to determine the design parameters of the water tank. According to the theory, it is known that the shallow water sloshing can be explained as the water level of the water tank is lower than  $1/3$  of the plate height of the water tank in the vibration direction; meanwhile, in the experiment, the optimal water level is 2 cm, the corresponding ratio is  $1/11$ , and the lesser amount of water cannot fill the tank uniformly. For the comprehensive analysis, it has been suggested that the 2–4 cm water level can be adopted for the good seismic performance, namely the water level should constitute  $1/11$  to  $1/10$  of the plate height in the vibration direction.

### 6. Conclusions and Outlooks

This study conducts an experiment to research the application of the integral water tank in the seismic performance of the slender structure. Several designed parameters, such as placement location and the height of the water level, are examined. Meanwhile, we also observe the sloshing characteristics of the water, and the experimental phenomenon is analyzed and discussed theoretically and experimentally. Finally, aiming at the design of the tank, we summarize a useful guide for the same or similar situation. According to the comparison and analysis of the experimental phenomenon, we can draw several conclusions as follows:

- (1) The installation of the integral water tank causes an obvious attenuation in the structural acceleration responses and the maximum acceleration amplitude, and the first natural frequency declines, which means the existence of the tank applies significant effects on the structural vibration characteristics.
- (2) The experimental vibration process suggests that the energy dissipation is mainly realized through the wave motion of the water and the reaction and the impact of the occurred swell, leading to the suppression in the structural vibration. In addition, the excitation of the external force and the different water level cause the diverse initial forms of the water, suggesting there are various waveforms of the water in the tank in the first stage; however, the final oscillation characteristics of the water achieve good consistency in the stable status.
- (3) The placement location of the water tank has a key influence on the energy dissipation. The higher of the placement, the more violent of the vibration amplitude and the acceleration, the more intense of the water motion, so that more energy can be absorbed.
- (4) The change in the water level illustrates a correlation to the structural damping. Compared to other floors, there is an obvious increase in the calculated damping based on the collected acceleration from the tank floor, and the placement on the top floor obtains optimal seismic performance. Meanwhile, the water tank with a water level of 4 cm on the top floor can achieve the maximum damping, followed by the water level of 2 cm.

Regarding the outlooks, there are two limitations that need to be further studied in the future. For instance, although the water motion characteristics are observed well due to the transparency of the acrylic material, the displacement of each floor is not measured. In addition, only the top and tank floors are measured due to the inadequate acceleration sensors, which cannot completely reflect the distribution of the structural vibration.

**Author Contributions:** Conceptualization B.X. and X.X.; Funding acquisition X.X.; Investigation Z.H., L.W. and H.C.; Methodology B.X. and Z.H.; Project administration B.X. and Z.H.; Resources Z.H., L.W., Q.L. and H.C.; Supervision B.X. and X.X.; Validation Q.L. and H.C.; Visualization L.W. and Q.L.; Writing—original draft Z.H., L.W. and Q.L.; Writing—review & editing B.X., X.X. and H.C. All authors have read and agreed to the published version of the manuscript.

**Funding:** This work is supported by Open Fund of Key Laboratory of Navigation Structures Technology, Ministry of Transport (NO. 8190011).

**Data Availability Statement:** Not applicable.

**Conflicts of Interest:** The authors declare no conflict of interest.

## References

1. Bandyopadhyay, R.; Maiti, S.; Ghosh, A.D.; Chatterjee, A. Overhead water tank shapes with depth-independent sloshing frequencies for use as TLDs in buildings: Overhead water tank shapes with depth-independent sloshing frequencies. *Struct. Control. Health Monit.* **2018**, *25*, e2049. [[CrossRef](#)]
2. Hu, X.; Zhao, Z.; Weng, D.; Hu, D. Design of a pair of isolated tuned liquid dampers (ITLDs) and application in multi-degree-of-freedom structures. *Int. J. Mech. Sci.* **2021**, *217*, 107027. [[CrossRef](#)]
3. Konar, T.; Ghosh, A. A review on various configurations of the passive tuned liquid damper. *J. Vib. Control.* **2022**. [[CrossRef](#)]
4. Ocaik, A.; Nigdeli, S.M.; Bekdaş, G.; Kim, S.; Geem, Z.W. Adaptive Harmony Search for Tuned Liquid Damper Optimization under Seismic Excitation. *Appl. Sci.* **2022**, *12*, 2645. [[CrossRef](#)]
5. Konar, T.; Ghosh, A.D. Flow Damping Devices in Tuned Liquid Damper for Structural Vibration Control: A Review. *Arch. Comput. Methods Eng.* **2020**, *28*, 2195–2207. [[CrossRef](#)]
6. Zhang, Z. Numerical and experimental investigations of the sloshing modal properties of sloped-bottom tuned liquid dampers for structural vibration control. *Eng. Struct.* **2019**, *204*, 110042. [[CrossRef](#)]
7. Banerji, P.; Murudi, M.; Shah, A.H.; Popplewell, N. Tuned liquid dampers for controlling earthquake response of structures. *Earthq. Eng. Struct. Dyn.* **2000**, *29*, 587–602. [[CrossRef](#)]
8. Pirner, M.; Urushadze, S. Liquid damper for suppressing horizontal and vertical motions—Parametric study. *J. Wind. Eng. Ind. Aerodyn.* **2007**, *95*, 1329–1349. [[CrossRef](#)]
9. Sun, L.M.; Fujino, Y.; Pacheco, B.M.; Isobe, M. Nonlinear waves and dynamic pressures in rectangular tuned liquid damper (tld): Simulation and experimental verification. *Doboku Gakkai Ronbunshu* **1989**, *1989*, 81–92. [[CrossRef](#)]
10. Suthar, S.J.; Jangid, R.S. Design of tuned liquid sloshing dampers using nonlinear constraint optimization for across-wind response control of benchmark tall building. *Structures* **2021**, *33*, 2675–2688. [[CrossRef](#)]
11. Ghaemmaghami, A.; Kianoush, R.; Yuan, X.-X. Numerical Modeling of Dynamic Behavior of Annular Tuned Liquid Dampers for Applications in Wind Towers: Numerical modeling of dynamic behavior. *Comput.-Aided Civ. Infrastruct. Eng.* **2013**, *28*, 38–51. [[CrossRef](#)]
12. Gholamipoor, M.; Ghiasi, M. Numerical analysis of fully non-linear sloshing waves in an arbitrary shape tank by meshless method. *Eng. Anal. Bound. Elem.* **2022**, *144*, 366–379. [[CrossRef](#)]
13. Drosos, J.; Tsinopoulos, S.; Karabalis, D. Seismic retrofit of spherical liquid storage tanks with energy dissipative devices. *Soil Dyn. Earthq. Eng.* **2019**, *119*, 158–169. [[CrossRef](#)]
14. Akyıldız, H.; Ünal, N.E.; Aksoy, H. An experimental investigation of the effects of the ring baffles on liquid sloshing in a rigid cylindrical tank. *Ocean Eng.* **2013**, *59*, 190–197. [[CrossRef](#)]
15. Kwon, D.K.; Kareem, A. Hybrid simulation of a tall building with a double-decker tuned sloshing damper system under wind loads. *Struct. Des. Tall Spec. Build.* **2020**, *29*, e1790. [[CrossRef](#)]
16. Das, A.; Maity, D.; Bhattacharyya, S.K. Investigation on the efficiency of deep liquid tanks in controlling dynamic response of high-rise buildings: A computational framework. *Structures* **2022**, *37*, 1129–1141. [[CrossRef](#)]
17. Zheng, J.; Dou, P.; Xue, M.-A. Dynamics coupling analysis between elastic supporting structure and TLD with and without slat screen. *Structures* **2022**, *46*, 969–987. [[CrossRef](#)]
18. Ashasi-Sorkhabi, A.; Malekghasemi, H.; Ghaemmaghami, A.; Mercan, O. Experimental investigations of tuned liquid damper-structure interactions in resonance considering multiple parameters. *J. Sound Vib.* **2017**, *388*, 141–153. [[CrossRef](#)]
19. Behbahani, H.P.; bin Adnan, A.; Vafaei, M.; Shad, H.; Pheng, O.P. Vibration Mitigation of Structures through TLCD with Embedded Baffles. *Exp. Tech.* **2016**, *41*, 139–151. [[CrossRef](#)]

20. Malekghasemi, H.; Ashasi-Sorkhabi, A.; Ghaemmaghami, A.R.; Mercan, O. Experimental and numerical investigations of the dynamic interaction of tuned liquid damper–structure systems. *J. Vib. Control*. **2013**, *21*, 2707–2720. [[CrossRef](#)]
21. Vandiver, J.; Mitome, S. Effect of liquid storage tanks on the dynamic response of offshore platforms. *Appl. Ocean Res.* **1979**, *1*, 67–74. [[CrossRef](#)]
22. Koh, C.G.; Mahatma, S.; Wang, C.M. Theoretical and experimental studies on rectangular liquid dampers under arbitrary excitations. *Earthq. Eng. Struct. Dyn.* **1994**, *23*, 17–31. [[CrossRef](#)]
23. Jin, Q.; Li, X.; Sun, N.; Zhou, J.; Guan, J. Experimental and numerical study on tuned liquid dampers for controlling earthquake response of jacket offshore platform. *Mar. Struct.* **2007**, *20*, 238–254. [[CrossRef](#)]
24. Chen, X.; Wang, L.; Xu, J. TLD Technique for Reducing Ice-Induced Vibration on Platforms. *J. Cold Reg. Eng.* **1999**, *13*, 139–152. [[CrossRef](#)]
25. Nakamura, S.-I.; Kawasaki, T. Lateral vibration of footbridges by synchronous walking. *J. Constr. Steel Res.* **2006**, *62*, 1148–1160. [[CrossRef](#)]
26. Kareem, A.; Sun, W.-J. Stochastic response of structures with fluid-containing appendages. *J. Sound Vib.* **1987**, *119*, 389–408. [[CrossRef](#)]
27. Toshiyuki, N.; Tanaka, Y. Study on a Vibration Damper System Using Hydrodynamic Force of Sloshing: Part 4. Vibration Tests of Model Tanks. In *Summaries of Technical Papers of Annual Meeting Architectural Institute of Japan*; B, Structures I; Architectural Institute of Japan: Tokyo, Japan, 1988.
28. Fediw, A.A.; Isyumov, N.; Vickery, B.J. Performance of a tuned sloshing water damper. *J. Wind. Eng. Ind. Aerodyn.* **1995**, *57*, 237–247. [[CrossRef](#)]
29. Roy, A.; Zhang, Z.; Ghosh, A.; Basu, B. On the nonlinear performance of a tuned sloshing damper under small amplitude excitation. *J. Vib. Control*. **2019**, *25*, 2695–2705. [[CrossRef](#)]
30. Roy, A.; Staino, A.; Ghosh, A.; Basu, B.; Chatterjee, S. Seismic Vibration Control of Elevated Water Tank by TLD and Validation of Full-Scale TLD Model through Real-Time-Hybrid-Testing. *J. Phys. Conf. Ser.* **2016**, *744*, 012042. [[CrossRef](#)]
31. Ocaik, A.; Bekdaş, G.; Nigdeli, S.M.; Kim, S.; Geem, Z.W. Optimization of Tuned Liquid Damper Including Different Liquids for Lateral Displacement Control of Single and Multi-Story Structures. *Buildings* **2022**, *12*, 377. [[CrossRef](#)]
32. Zhang, Z. Understanding and exploiting the nonlinear behavior of tuned liquid dampers (TLDs) for structural vibration control by means of a nonlinear reduced-order model (ROM). *Eng. Struct.* **2022**, *251*, 113524. [[CrossRef](#)]
33. Kamgar, R.; Gholami, F.; Sanayei, H.R.Z.; Heidarzadeh, H. Modified Tuned Liquid Dampers for Seismic Protection of Buildings Considering Soil–Structure Interaction Effects. *Iran. J. Sci. Technol. Trans. Civ. Eng.* **2019**, *44*, 339–354. [[CrossRef](#)]
34. Zhao, Z.; Hu, X.; Chen, Q.; Wang, Y.; Hong, N.; Zhang, R. Friction pendulum-strengthened tuned liquid damper (FPTLD) for earthquake resilience of isolated structures. *Int. J. Mech. Sci.* **2022**, *244*, 108084. [[CrossRef](#)]
35. Hsieh, M.-C.; Huang, G.-L.; Liu, H.; Chen, S.-J.; Chen, B.-F. A numerical study of hybrid tuned mass damper and tuned liquid damper system on structure motion control. *Ocean Eng.* **2021**, *242*, 110129. [[CrossRef](#)]

**Disclaimer/Publisher’s Note:** The statements, opinions and data contained in all publications are solely those of the individual author(s) and contributor(s) and not of MDPI and/or the editor(s). MDPI and/or the editor(s) disclaim responsibility for any injury to people or property resulting from any ideas, methods, instructions or products referred to in the content.